Evaluation of Stability and Flying Qualities of a Light Unmanned Aerial Vehicle (UAV)

Mikael Samuelsson

August 2, 2012

Abstract

The objective of this study was to evaluate the flying qualities of a light unmanned aerial vehicle (UAV) developed by the Thai company AVIA Satcom Co., Ltd. Based on the study changes in design was to be suggested to meet stability requirements and recommendations from European Aviation Safety Agency and Federal Aviation Administration. The evaluation was based on two different analyses. First, the stability characteristics in terms of stability modes were examined by creating a flight dynamics model of the studied airplane. Secondly the controllability of the vehicle was investigated by examining the control surfaces. It was found that the original design of the UAV was dynamically unstable and that the control surfaces were too large making the airplane difficult to fly in trim condition. By studying the stability characteristics of the simulated airplane it could be concluded that the UAV was dynamically stable for the improved design and thereby meet the requirements and recommendations.

Nomenclature

Ph	Phugoid Mode	L	Lift Force	α	Angle of Attack
Sp	Short Period Mode	D	Drag Force	β	Angle of Side Slip
DR	Dutch Roll Mode	Y	Side Force	ϕ	Roll Angle
R	Rolling Convergence Mode	W	Weight of the UAV	θ	Pitch Angle
Spi	Spiral Mode	l	Roll Moment	ψ	Yaw Angle
x_{pos}	x-position (Body)	M	Pitch Moment	x	State Vector
y_{poz}	y-position (Body)	n	Yaw Moment	$\dot{x}$	Derivative State Vector
y_E	y-position (Earth)	C_L	Lift Force Coefficient	ρ	Density of Air
z_{pos}	z-position (Body)	C_D	Drag Force Coefficient	mf	Fuel Mass
u	Airspeed in x_{pos}-direction	C_Y	Side Force Coefficient	δ_a	Aileron Deflection
v	Airspeed in y_{pos}-direction	C_l	Roll Moment Coefficient	δ_e	Elevator Deflection
w	Airspeed in z_{pos}-direction	C_M	Pitch Moment Coefficient	δ_r	Rudder Deflection
V_∞	True Airspeed	C_n	Yaw Moment Coefficient	δ_T	Trottle Position
p	Roll Rate	I_x	Moment of Inertia (x)	A_{long}	Longitudial System Matrix
q	Pitch Rate	I_y	Moment of Inertia (y)	A_{lat}	Lateral System Matrix
r	Yaw Rate	I_z	Moment of Inertia (z)	J	Jacobian Matrix
$\bar{p}$	Non dimensional Roll Rate	$\dot{\bar{\alpha}}$	Non dimensional rate of α	LSF	Load Sensitivity Factor
$\bar{q}$	Non dimensional Pitch Rate	S	Wing Reference Area	n_{load}	Load Factor
$\bar{r}$	Non dimensional Yaw Rate	b	Wing Span	λ	Eigenvalue
ω	Natural Frequency	$t_{1/2}$	Time to Half Amplitude	T_R	Roll Mode Time Constant
ζ	Damping Ratio	$N_{1/2}$	Cycles to Half Amplitude	T_{Spi}	Min. Time to Double Amplitude

1 Introduction

An airplane's ability to operate safely is essential, independent of its purpose of flight. Whether it is a passenger jet transporting customers to various destinations or unmanned aerial vehicles (UAVs) recording video or delivering items, the airplane's design for stability and control is of paramount importance.

In early stages of design, linear mathematical models, describing the motion of the airplane, are useful tools to estimate its static and dynamic stability characteristics as well as handling performance.

AVIA Satcom Co., Ltd. is a Thai company developing and supplying high-tech products for telecommunication, with focus on aviation and defence. AVIA Satcom is currently developing an UAV and has recently completed an extensive conceptual study of a high aspect ratio, boom tailed airplane. Statistical methods were used for the initial design and sizing of horizontal and vertical stabilizers as well as control surfaces. The study was based on statistical and historical data. As a second stage in their research, a detailed stability and control analysis will be necessary.

The objective with this project is to conduct such a study to evaluate the static and dynamic stability of the UAV. One of the main objectives is to suggest improvements in the design of the UAV such that the stability criteria or recommendations from European Aviation Safety Agency (EASA) [13] and Federal Aviation Administration (FAA) [14] are met without extensive changes in the layout or design [19].

The analysis will be carried out on a prototype which will be a half scale model of the final product. AVIA Satcom refers to the half scale prototype as "The Black Kite". We will, throughout the remainder of the this report, also refer to the prototype as "The Black Kite".

2 Background

2.1 The Studied UAV

The studied UAV (*The Black Kite*) is AVIA's preliminary design based on a previous extensive conceptual design study carried out at the company. The initial design proposal of the UAV is a small, light weight, high aspect ratio design with a twin-boom configuration propelled by a pusher-propeller. The propeller is powered by a $14\,kW$ single piston four-stroke engine. The airfoil selection for the Black Kite is an Eppler 407 for the main wing with a tapered trailing edge along the entire wing span, flaps included and no dihedral. For both the horizontal and vertical stabilizers the NACA 0012 airfoil is used with no dihedral. The horizontal stabilizer is mounted with a 3° negative inclination angle (negative angle meaning leading edge lower than trailing edge of the horizontal stabilizer). The UAV will have a maximum take-off mass of $58\,kg$ (See *Table* 8 or *Table* 9 in *Appendix A*) capable of carrying a selection of different payloads limited to a maximum of $20\,kg$. The desired payload will be a high-technology camera for monitoring areas and objects of interest. [16, 17]. It is expected that the Black Kite will operate within a speed range of $30\,m/s$ to $40\,m/s$ at an altitude of $2000\,feet$ to $6000\,feet$ above sea level. Further design details of the Black Kite can be found in *Appendix A*.

The static and dynamic stability response characteristics and the handling qualities were determined using the derived data, the stability derivatives estimates [18] along with the design features from the previous study. This was done by modelling the UAV using *Euler's equations of motion* [4]. The stability derivatives are also found in *Appendix A*.

2.2 Aircraft Requirements and Recommendations

When designing an airplane it has to be constructed to meet a set of requirements to prove airworthiness and to ensure safety when operating. The requirements of airworthiness and safety are based on knowledge and information by two agencies whose main function is to determine regulations on how to design the important parts of an aircraft. The two agencies are EASA [13] and FAA [14].

The requirements involving forces restricted by human limitations will not be considered since the studied airplane is unmanned and the control manoeuvres usually carried out by a pilot are now executed by power servos. The regulations by EASA and FAA will be supplemented with recommendations to serve as a base for the study of handling and stability.

2.3 EASA/FAA

The requirements used in this study were taken from EASA's "Certification Specifications for Very Light Aeroplanes CS-VLA" [13] that coincides with the regulations and requirements from FAA. The recommendations to compliment the requirements were taken from U.S. Department of Defence's Regulations Military Specification - "Flying Qualities of Piloted Airplanes, MIL-F-8785C" [15]. Applicability conditions for the airworthiness code of CS-VLA

are stated in *Appendix G*. The studied UAV meet the requirements for applicability of the CS-VLA, see *Table* 5 in *Appendix A*.

Stability requirements will be investigated along with stability recommendations which will serve as a supplement due to insufficient information about the requirements and because some requirements have been neglected since the regulations are based on a manned aircraft. The requirements and the recommendations can be found in *Appendix G*.

2.4 Classification of the UAV

One of the main objectives of this study was to analyze the stability characteristics of the five different stability modes; *Phugoid, Short Period, Dutch Roll, Rolling Convergence* and *Spiral mode*. The characteristics in terms of damping, natural frequency and time constants corresponding to each mode were then to be compared to requirements imposed by EASA and FAA along with MIL-F-8785C recommendations on the dynamic behaviour.

MIL-F-8785C is based on different classes, categories and levels of airplanes and flight phases, with different recommendations. For MIL-F-8785C the Black Kite will serve under *Class* 1; small light airplanes, *Category B*; climb, cruise, loiter and descent. Furthermore, there are three different levels of stability stated in MIL-F-8785C; *Level* 1, *Level* 2 and *Level* 3. Since the Black Kite is unmanned, *Level* 1 and *Level* 2 can be seen as the same level. Despite this, since *Level* 1 has stricter limitations and therefore will result in better flying qualities, the UAV will be designed to be as close to *Level* 1 as possible. It should be said that with better flying qualities it is meant that; the behaviour and the controllability of the airplane is adequate for completing the mission without any complications. This is different for different kind of airplanes. For an UAV whose main mission is to cruse at high altitudes recording video a stable airplane is necessary which is less sensitive to rudder deflection to keep a steady heading. On the other hand when designing a fighter jet a unstable airplane is often desired to give low response time and good manoeuvrability. Definitions of the different *Classes*, *Categories* and *Levels* can be found in *Appendix G*.

3 Method

3.1 Flight Dynamics Model

A mathematical model of the Black Kite was created to investigate and evaluate the physical forces acting on the simulated aircraft, such as thrust, lift and drag together with momentum about the airplane body axes. By modelling the UAV information about the stability characteristics could be obtained. The model is based on a set of mathematical equations and on aerodynamic data supplied by AVIA. The model was coded using Matlab [20].

3.2 Model Build Up

The airplane model that will simulate UAV's motion is built up of several equations known as Euler's Equations of Motion. These equations are based on aerodynamic forces, moments acting on the airplane and properties of the vehicle. These are commonly used to model the movement of an airplane. The aerodynamic forces were calculated using non-dimensional derivatives which describe the connection of the movement of the airplane to the physical forces acting on it. The estimated non-dimensional derivatives called aerodynamic coefficients were provided from a previous aerodynamic analysis study conducted by AVIA [18]. These coefficients are vehicle specific and are used to describe the aerodynamic behaviour of the simulated airplane of interest. Each part of the modelling was divided into separate sections to provide a good overview of the modelling. The main parts of the modelling of the UAV are the *aerodynamic properties, the equations of motion* and the *solver*. The solver uses the *aerodynamic properties and the equations of motion* to calculate the state forces.

3.2.1 Aerodynamic Properties

When modelling the UAV, the aerodynamic forces acting on the airplane must be known. These forces are calculated using the aerodynamic properties, earlier referred to as the aerodynamic coefficients, and the design layout of the UAV. Equations used in this study to describe the lift- , drag- and side-force are stated below along with the equations for the moments about the body axes of the UAV.

Lift force	$L = \frac{1}{2}\rho V^2 S C_L$	Roll moment	$l = \frac{1}{2}\rho V^2 S b C_l$
Drag force	$D = \frac{1}{2}\rho V^2 S C_D$	Pitch moment	$M = \frac{1}{2}\rho V^2 S b C_M$
Side force	$Y = \frac{1}{2}\rho V^2 S C_Y$	Yaw moment	$n = \frac{1}{2}\rho V^2 S b C_n.$

The coefficient denoted C is the total aerodynamic coefficients for each force or moment. These coefficients depend on the state of the airplane in terms of magnitude of angles, rate of change of the orientation of the airplane as well as control surface deflection. Each coefficient is built up by sub-coefficients that take these actions into account. *Equation* 1 to *Equation* 6 show the aerodynamic coefficients used in this analysis.

$$C_L = C_{L0} + C_{L\alpha} \cdot \alpha + C_{Lq} \cdot \bar{q} + C_{L\delta_a} \cdot \delta_a + C_{L\delta_e} \cdot \delta_e + C_{L\delta_f} \cdot \delta_f \tag{1}$$

$$C_D = C_{Dmin} + K \cdot (C_L - C_{Lmin})^2 \tag{2}$$

$$C_Y = C_{Y0} + C_{Y\alpha} \cdot \alpha + C_{Y\beta} \cdot \beta + C_{Yp} \cdot \bar{p} + C_{Yr} \cdot \bar{r} + C_{Y\delta_a} \cdot \delta_a + C_{Y\delta_r} \cdot \delta_r + C_{Y\alpha\delta_a} \alpha \cdot \delta_a \tag{3}$$

$$C_l = C_{l0} + C_{l\alpha} \cdot \alpha + C_{l\beta} \cdot \beta + C_{lp} \cdot \bar{p} + C_{lr} \cdot \bar{r} + C_{l\delta_a} \cdot \delta_a + C_{l\delta_r} \cdot \delta_r + C_{l\alpha\beta} \cdot \alpha \cdot \beta + C_{l\alpha\delta_r} \cdot \alpha \cdot \delta_r \tag{4}$$

$$C_M = C_{M0} + C_{M\alpha} \cdot \alpha + C_{Mq} \cdot \bar{q} + C_{M\delta_a} \cdot \delta_a + C_{M\delta_e} \cdot \delta_e + C_{M\delta_f} \cdot \delta_f + C_{M\dot{\alpha}} \cdot \bar{\dot{\alpha}} \tag{5}$$

$$C_n = C_{n0} + C_{n\alpha} \cdot \alpha + C_{n\beta} \cdot \beta + C_{np} \cdot \bar{p} + C_{nr} \cdot \bar{r} + C_{n\delta_a} \cdot \delta_a + C_{n\delta_r} \cdot \delta_r + C_{n\alpha\delta_a} \cdot \alpha \cdot \delta_a. \tag{6}$$

In AVIA's previous study many aerodynamic sub-coefficients were estimated along with their influence on forces and moments [18]. Among those, the sub-coefficients that had the greatest influence on the force or moment were used in this study. A description of the sub-coefficients can be found in *Appendix H*.

3.2.2 Equations of Motion

The aerodynamic forces calculated according to above were used together with Euler's equations of motion [4] to estimate the movement of the UAV. The variables used to describe the movement were; the velocity components in x_{pos}, y_{pos} and $z_{pos} - direction$; u, v and w, angle of orientation; roll angle ϕ; pitch angle θ and yaw angle ψ. Moreover, rate of roll, pitch and yaw; p, q and r as well as position in x_{pos}, y_{pos} and $z_{pos} - direction$ were used to derive the motion of the UAV. The deduction of these properties is described in the next Section; *Solving the Problem*.

3.3 Solving the Problem

To calculate the movement of the UAV, Euler's equations of motion were put into an equation system. Rewriting the equations the derivative states could be obtained, i.e the derivative of the three velocities, the three rates, the three angles of orientation and the three coordinate locations. The derivative states were described by a vector denoted $\dot{x}$. It should be noted that the derivative states are differentiated with respect to time thus cannot be used to model the airplane. Therefore the non-derivative states, denoted x, had to be calculated from the derivative state vector $\dot{x}$. This was done according to the following procedure.

$$\dot{x} = \begin{bmatrix} \dot{u} & \dot{v} & \dot{w} & \dot{p} & \dot{q} & \dot{r} & \dot{\phi} & \dot{\theta} & \dot{\psi} & \dot{x}_{pos} & \dot{y}_{pos} & \dot{z}_{pos} & \dot{\delta_T} & \dot{\delta_e} & \dot{\delta_a} & \dot{\delta_r} & \dot{mf} & \dot{V_\infty} & \dot{y_E} \end{bmatrix}^T \tag{7}$$

$$x = \begin{bmatrix} u & v & w & p & q & r & \phi & \theta & \psi & x_{pos} & y_{pos} & z_{pos} & \delta_T & \delta_e & \delta_a & \delta_r & mf & V_\infty & y_E \end{bmatrix}^T. \tag{8}$$

The two vectors $\dot{x}$ and x were set up as a state space system. See *Equation* 9.

$$\dot{x} = A \cdot x \tag{9}$$

where A is known as the system matrix which could only have the property of deriving the non-derivative state vector. A matrix with this property is called a Jacobian matrix. A vector multiplied with the Jacobian matrix turns into the derivative of that vector with respect to each variable in the specific vector.

To solve the state space system some important properties of $\dot{x}$ had to be defined. The analysis of the UAV was carried out in trimmed flight condition and since $\dot{x}$ describe the time derivatives of the state of the airplane some of these variables were conditioned to be zero. These variables were: body x_{pos}, y_{pos} and z_{pos} accelerations; $\dot{u}$, $\dot{v}$ and $\dot{w}$, the rates $\dot{p}$, $\dot{q}$ and $\dot{r}$ as well as time derivative of the altitude position. This means that the airplane has a steady and levelled flight without any accelerations. Note that extra properties have been added to the state vectors to control the properties that are conditioned to be zero.

Knowing the criteria of the derivative state vector the system matrix and the non-derivative state vector that satisfies these conditions can be calculated. The format of the Jacobian matrix is the following:

$$J = \begin{bmatrix} \frac{\delta x_1}{\delta x_1} & \cdots & \frac{\delta x_1}{\delta x_n} \\ \vdots & \ddots & \vdots \\ \frac{\delta x_n}{\delta x_1} & \cdots & \frac{\delta x_n}{\delta x_n} \end{bmatrix}. \tag{10}$$

The Jacobian matrix was derived by using Newton-Raphson's method for numerical derivation. Applying the properties of the Jacobian matrix on the two state vectors we can determine which non-derivative state variables we have to vary to make the predetermined derivative state vector properties go to zero. By inserting a initial estimation of x and looping this system until the predetermined states of $\dot{x}$ reach zero the system matrix and the trimmed x vector could be obtained. The system matrix could then be split into two separate system matrices; one for longitudinal motion and one for lateral motion for the studied UAV, named A_{long} and A_{lat}. From the system matrices A_{long} and A_{lat}, information of the longitudinal and lateral stability modes of the aircraft were generated by examining the eigenvalues of each matrix. The trimmed state vector and orientation of the aircraft were also used to determine the trimmed flight conditions of the UAV.

4 Results and Discussion

4.1 Data Analysis

Before the full analysis was carried out, the accuracy of the Flight Dynamics Model (FDM) had to be examined to verify that the calculations were correct. This was done by comparing the matrices generated from the numerical derivation to approximated longitudinal and lateral system matrices [4]. The approximated matrices, named $A_{long_{approx}}$ and $A_{lat_{approx}}$, are based on the linear equations of motion containing few assumptions [4] making the approximated system matrices easy to use while giving accurate enough results to use as a verification to the flight dynamics model.

To minimize difference from the full analysis with the approximations, the comparison was done at a velocity of $35\,m/s$ and at sea level altitude i.e. the same conditions used when estimating the aerodynamic properties, or aerodynamic coefficients, of the UAV. The position of the center of gravity was also placed at the same location used at the estimation. This is important since the approximated matrices are built up by raw aerodynamic data and would otherwise not give a accurate outcome to compare to the FDM. The build up of $A_{long_{approx}}$ and $A_{lat_{approx}}$ can be found in *Appendix F* along with the numerical values of both the approximations and the matrices generated from the flight dynamics model.

Since the dynamic stability analysis is based on the eigenvalues of each matrix, the FDM and approximated eigenvalues were compared with each other. Examining the longitudinal eigenvalues it was found that accuracy of the FDM is fairly high with only 0.50 % and 13.95 % error for the real part of $\lambda_{long1,2}$ and $\lambda_{long3,4}$, respectively and 0.37 % and 2.49 % error for the imaginary part of $\lambda_{long1,2}$ and $\lambda_{long3,4}$, respectively. When comparing the lateral eigenvalues it could be determined that the error of the real part of $\lambda_{lat1,2}$, λ_{lat3} and λ_{lat4} compared with the approximation is 0.005 %, 0.008 % and 3.04 %, respectively and the error of the imaginary part of $\lambda_{lat1,2}$ is 0.002 %. See *Table* 16 in *Appendix F* for complete comparison. The highest difference of the comparison is the 13.95 % error of the real part of the third and fourth eigenvalue. The approximations are simplifications of the full analysis and are therefore not as accurate as the full analysis itself [4] why the comparison between the approximated and the FDM generated eigenvalues is not a 100 % match.

Secondly, before the complete analysis was made the flight dynamics model was compared to a flight simulator at AVIA. The flight simulator is based on the well known flight model "JSBsim" [21] and simulated using a simulation tool named "Flight Gear" [22]. The two models were compared at trimmed flight condition at 2000 $feet$ altitude, $35\,m/s$ airspeed using the aerodynamic data for the Black Kite. Numerical data extracted from both simulations were found to match. The data extracted were; the magnitude of thrust, the lift, the drag, the momentum as well as the control surface deflection and the angle of attack.

As a third step prior to the analysis the ambient conditions had to be determined. In the Section "The studied UAV" it is stated that the Black Kite will operate within a speed range of $30\,m/s$ to $40\,m/s$ at an altitude from 2000 $feet$ to 6000 $feet$ above sea level. Since one of the main objectives of this analysis was to examine the dynamic stability and suggest design improvements, the "worst case" ambient scenario, meaning the ambient scenario resulting in lowest stability, had to be determined. This was done by examining the eigenvalues of the longitudinal and lateral system matrices knowing that eigenvalues with negative real part have a stable behaviour and eigenvalues with positive real part have a unstable behaviour . The imaginary part (if present) can be translated

as the natural frequency. Have in mind that both the spiral mode and the rolling convergence mode are not of oscillating type and therefore have no oscillating movement, i.e. no imaginary part of the eigenvalue.

By plotting the variation of the real and imaginary parts of each eigenvalue (Root Locus Plot) with variation in airspeed and altitude, from the longitudinal and lateral system matrices, the tendency for dynamic stability could be determined.

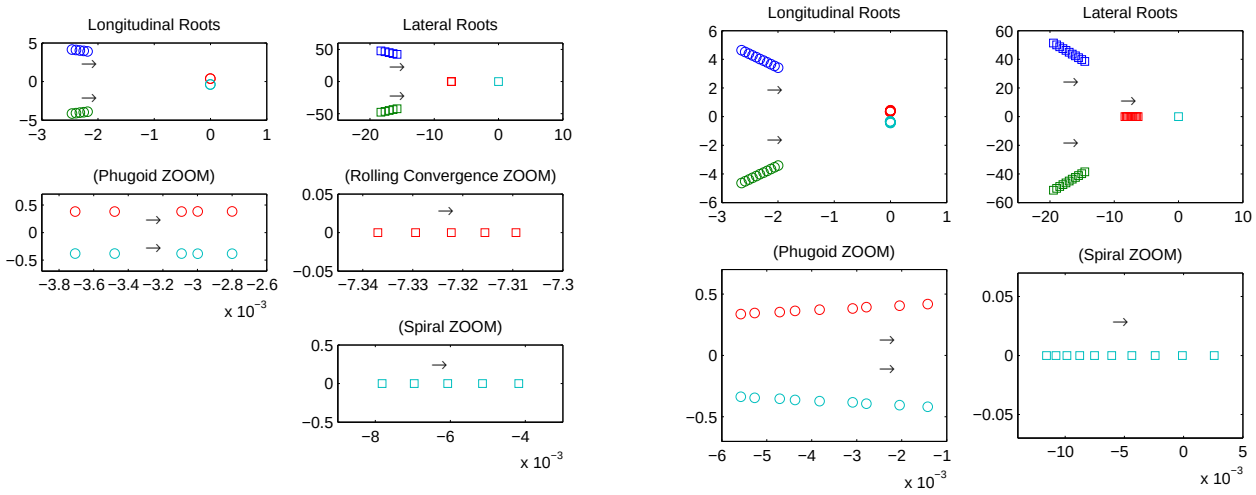

Circle: Green/Blue = SP, Red/Turquoise = Ph.
Square: Green/Blue = DR, Red = R, Turquoise = Spi.

Figure 1: Root locus of Longitudinal and Lateral Eigenvalues
(Left: Altitude variation 2000 $feet$ to 6000 $feet$ | Right: Airspeed variation 40 m/s to 30 m/s)

From the root locus plot we can see that dynamic stability is reduced for all stability modes with increasing altitude and with decreasing airspeed. From the root locus it was thus determined that the "worst case" ambient scenario for the UAV was when operating at an altitude of 6000 $feet$ and at an airspeed of 30 m/s. Due to above conclusions, further analysis was conducted at the "worst case" scenario environment within the expected operating limits.

In Section 2 it is mentioned that the UAV must be capable to carry a selection of different payloads depending on the current mission. The selection of payload has been assumed to be two different cameras suitable for an UAV; the 3 kg T-stamp camera and the 11.5 kg SHAPO camera from the manufacturer Controp [23]. The analysis has therefore been conducted with the two likely payloads for the UAV. The variation of payload have been simulated by varying the payload mass giving a total of six different flight scenarios, including the non-payload case. The flight scenarios have been compiled in *Table* 1.

To have sufficient distribution of mass a balance weight was used to give enough static margin. A static margin of $5-15\%$ of the mean aerodynamic chord is desirable [3] to have proper static stability and still have sufficient manoeuvrability meaning not to slow "reaction" time. Low static margin is also desirable to avoid trim drag to minimize fuel consumption. A table of static margin corresponding to payload can be found in *Appendix B*.

Table 1: Likely Flight Scenarios of the Black Kite (Original Design)

$Fligh\,Scenario$	$Payload\,[kg]$	$Fuel\,Weight\,[kg]$	$Balance\,Weight\,[kg]$
1	0 $(Min.)$	6	3.5
2	0 $(Min.)$	0	3.5
3	3 $(T-Stamp)$	6	2.5
4	3 $(T-Stamp)$	0	2.5
5	11.5 $(SHAPO)$	6	0
6	11.5 $(SHAPO)$	0	0

All weights are in [kg]

4.2 Dynamic Stability

The dynamic stability for all different flight scenarios were investigated in terms of damping ratio, natural frequency and time constants. These parameters were extracted from the system matrices generated from the FDM. Firstly the original design of the UAV was analyzed and compared with EASA's and FAA's requirements as well as the MIL-F-8785C recommendations. The scenario with highest quantity of worst dynamic stability was determined to appear in flight scenario 5. Despite this, flight scenario 4 was chosen to be the overall worst dynamic case. This is due to when comparing the characteristics available in the requirements and recommendations. With scenario 5 we can see that none of the characteristics are critical unlike the Phugoid damping in scenario 4 which is negative and does not satisfy the recommended limit. See *Table* 2 for dynamic characteristics for scenario 4. For complete analysis (all scenarios) see *Table* 12 and 13 in *Appendix C*.

Table 2: Dynamic Stability Characteristics (Scenario 4, Original Design)

Longitudinal		*Value*	*Unit*	*Lateral*		*Value*	*Unit*
	ω_{SP}	3.48	$[rad/s]$		ω_{DR}	38.33	$[rad/s]$
	ζ_{SP}	0.52	$[-]$		ζ_{DR}	0.36	$[-]$
Short Period	LSF	7.29	$[g's/rad]$	*Dutch Roll*	$\omega_{DR} \cdot \zeta_{DR}$	13.97	$[rad/s]$
	$t_{1/2_{SP}}$	0.35	$[s]$		$t_{1/2_{DR}}$	0.05	$[s]$
	$N_{1/2_{SP}}$	0.18	$[cycles]$		$N_{1/2_{DR}}$	0.28	$[cycles]$
	ω_{Ph}	0.43	$[rad/s]$	*Rolling Conv.*	T_R	0.16	$[s]$
Phugoid	ζ_{Ph}	-0.0048	$[-]$				
	$t_{1/2_{Ph}}$	-331.84	$[s]$				
	$N_{1/2_{Ph}}$	-22.85	$[cycles]$	*Spiral*	T_{Spi}	404.47	$[s]$

Generated at true airspeed $30\,m/s$ at $6000\,feet$ altitude. (Negative time- and cycle to half amplitude indicate time- and cycle to double amplitude due to negative damping)

The critical stability mode can obviously be seen to be the Phugoid mode behaviour since the real part of its eigenvalue is positive resulting in a negative damping of the motion. Generally, there are three properties that effects the phugoid mode stability of an airplane; drag, lift and center of gravity position (Static Margin). From [1] it is known that the damping of the Phugoid mode can be approximated according to *Equation* 11 for a stable airplane.

To increase the damping of the Phugoid mode, either drag D could be increased or lift L could be decreased. But since a high lift to drag ratio is one of the main objectives of airplane design, especially for a high aspect ratio powered glider as the Black Kite, neither of the proposed actions are satisfying. It is therefore easy to understand why the damping of the Phugoid mode is usually very low, as can be seen in this case. The third action that could be taken to enhance the stability of the Phugoid mode is by moving the position of the center of gravity to keep sufficient static margin while adding weight to the airplane. This can be compared to ballast weight placed in the lower parts of a boat or ship to make it stable. Further examination of the short period frequency compared to the recommendations of MIL-F85687C shows that the recommendation for *Level* 1 stability is met though being close to *Level* 2 characteristics. This can be seen in the left graph in *Figure* 2, where the short period frequency is plotted against the "Load Sensitivity Factor" n_{load}/α, defined in *Equation* 12 [24]. The load sensitivity factor describe the change in load factor with change in angle of attack.

$$\zeta_{Phugoid} = \frac{1}{\sqrt{2}} \frac{D}{L}. \tag{11}$$

$$n_{load}/\alpha = \frac{\bar{q} C_{L_\alpha}}{W/S}. \tag{12}$$

Since the short period mode is one of the two longitudinal motions the stability characteristics can be modified by changing the location of the center of gravity. Since the critical stability mode was the Phugoid, the high priority was to make this mode stable within the highest level as possible while keeping the fairly good characteristics of the short period mode. This was done by relocating the center of gravity to increase or decrease the static margin. By adding an extra balance weight in the aft of the UAV this could be achieved. The change of static margin was done within the limits of $5-15\%$ of the mean aerodynamic chord as mentioned before. Unlike the original design, with the improved design i.e. relocated distribution of mass, it was possible to obtain proper static margin within

the limits while keeping the recommendations for the short period mode, *Figure.* 2, as well as making the Phugoid stable. The UAV's Phugoid mode was found to be stable in all scenarios for the mass distribution in *Table.* 9 in *Appendix A*.

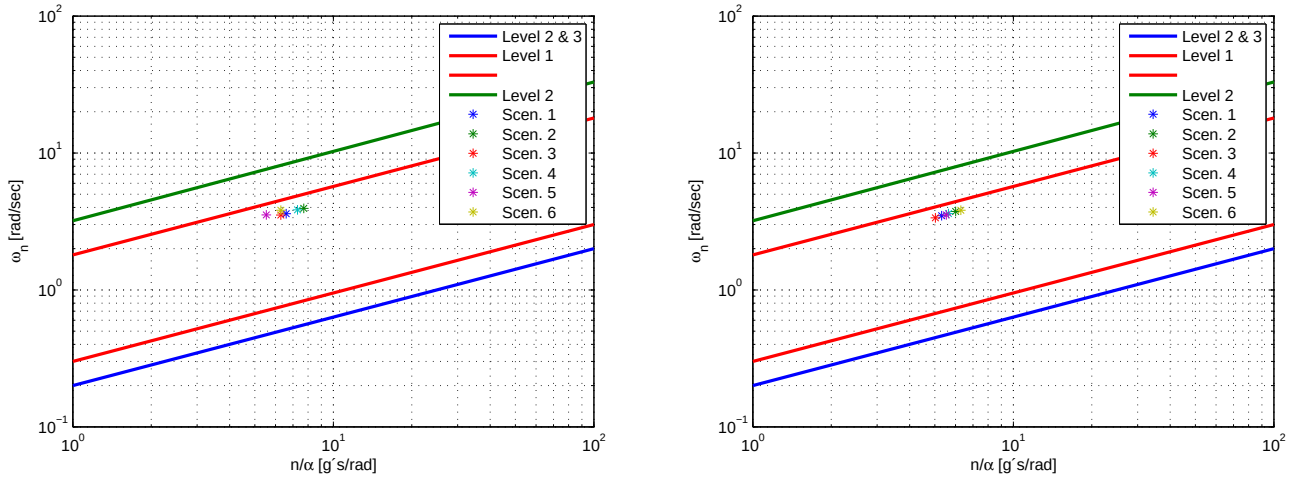

Figure 2: Short Period frequency requirements - Category B Flight Phases.
(Left: Original Design | Right: Improved Design)

See *Table* 8 and *Table* 9 in *Appendix A* for comparison between the old and new design. When comparing the dynamic characteristics from the different scenarios of the improved design of the Black Kite in *Table* 14 and *Table* 15 in *Appendix C* with the recommendations

MIL-F-8785C and requirements from EASA and FAA we can see that each scenario has different characteristics that are worse than others. Further analysis of the dynamic stability of the modified design we notice that the most critical scenario is when carrying only a payload of 11.5 kg with no fuel weight (end of mission) i.e. scenario number 6. This scenario is shown in *Table* 4. Examining the dynamic characteristics of flight scenario 6 we can see that the requirements are met for *Level* 1 recommendations *flight phase B*, except the Phugoid damping. The worst Phugoid damping of the full analysis appear in scenario 6 with a damping of $\zeta_{Ph} = 0.0008$. However the worst damping ratio satisfies the recommendations of *Level* 2 criteria which limits the damping to a minimum of zero, meaning that the airplane is stable for the new design. The positive stabillity is illustrated in *Figure* 3 where the two longitudinal modes step response is plotted for a unit step in α. In the left graph of *Figure* 3 the step response of the short period mode is illustrated.

Fligh Scenario	*Payload*	*Fuel Weight*	*Bal. Weight Nose*	*Bal. Weight Aft*
1_{change}	0 $(Min.)$	6	4.5	9
2_{change}	0 $(Min.)$	0	4.5	9
3_{change}	3 $(T - Stamp)$	6	3.5	10
4_{change}	3 $(T - Stamp)$	0	3.5	10
5_{change}	11.5 $(SHAPO)$	6	0	0
6_{change}	11.5 $(SHAPO$	0	0	0

All weights are in [kg]

From *Table* 4 we can see that the damping of the short period mode is 0.49 which is a high value of damping. Due to the high damping the oscillating movement of the short period mode in *Figure* 3 is not visible**.** In the right graphs of *Figure* 3 the Phugoid mode is plotted. As can be seen, both from *Table* 4 and *Figure* 3 the damping of the Phugoid mode is very low. The lower right graph however shows that the oscillating movement decays with time.

Table 3: Dynamic Stability Characteristics (Scenario 6 , Improved Design)

Longitudinal		*Value*	*Unit*	*Lateral*		*Value*	*Unit*
	ω_{SP}	3.82	$[rad/s]$		ω_{DR}	38.75	$[rad/s]$
	ζ_{SP}	0.49	$[-]$		ζ_{DR}	0.35	$[-]$
Short Period	LSF	6.29	$[g's/rad]$	*Dutch Roll*	$\omega_{DR} \cdot \zeta_{DR}$	13.53	$[rad/s]$
	$t_{1/2_{SP}}$	0.37	$[s]$		$t_{1/2_{DR}}$	0.05	$[s]$
	$N_{1/2_{SP}}$	0.19	$[cycles]$		$N_{1/2_{DR}}$	0.30	$[cycles]$
	ω_{Ph}	0.45	$[rad/s]$	*Rolling Conv.*	T_R	0.16	$[s]$
Phugoid	ζ_{Ph}	0.0008	$[-]$				
	$t_{1/2_{Ph}}$	1894.62	$[s]$				
	$N_{1/2_{Ph}}$	135.53	$[cycles]$	*Spiral*	T_{Spi}	79.20	$[s]$

Generated at true airspeed $30\,m/s$ at $6000\,feet$ altitude. (Negative time- and cycle to half amplitude indicate time- and cycle to double amplitude due to negative damping)

4.3 Static Stability

The UAV has now a stable design and meet the requirements and recommendations for the dynamic characteristics. The next step in the analysis was to examine the flying qualities. This was done by analyzing the static stability as well as the controllability of the UAV.

The static stability of an airplane is typically referred to as the pitching moment variation with angle of attack, α. *Figure* 4 illustrates the pitching moment versus α for different center of gravity positions, i.e. different flight scenarios. If the UAV would be affected by a pitching disturbance, such as a vertical gust and thereby experience a decrease in α, the layout of the airplane design would alter a positive pitching moment to counter the nose down movement, restoring the airplane to its equilibrium. It should be stated that a positive pitching moment is defined as a nose up movement, i.e. positive α. If the UAV then would receive a disturbance giving a nose up movement (increase in α), the airplane would produce a negative pitching movement restoring the airplane to its former equilibrium. Another important feature in static stability is the neutral point and the static margin which have been discussed in previous Sections. Results of the static margin of the improved design for different flight scenarios can be found in *Appendix B*, *Table* 11.

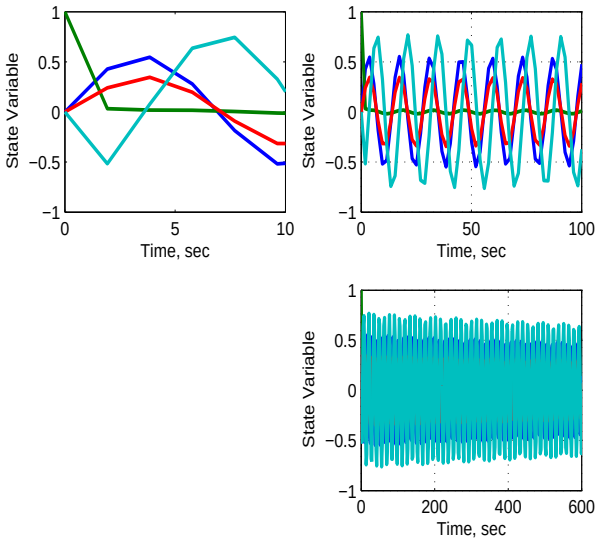

Blue $= V_\infty$, **Green** $= \alpha$, **Red** $= q$, **Turqoise** $= \theta$

Figure 3: Longitudinal Step Responce for a unit step in angle of attack. Left graph: Sp mode. Right Graphs: Ph mode (Scenario 6).

4.4 Flying Qualities

The flying qualities of an airplane are strongly connected to its control surfaces, both in size of area and angle of deflection. Below the acquired deflection in elevator, aileron and rudder are plotted against airspeed within the estimated range, to keep the UAV in trimmed condition at $4000\,feet$. Trimmed condition meaning the momentum about the body axes of the airplane and the rates of change of the UAV are zero with no change in altitude or airspeed. From the graphs in *Figure* 5 we can see that three control surfaces operate within a small interval of deflection, especially the rudders. This will difficult the use of the control surfaces by making the UAV more sensitive to disturbances in control surface deflection. Moreover, deflection with this precision is difficult to achieve even though operated by power servos.

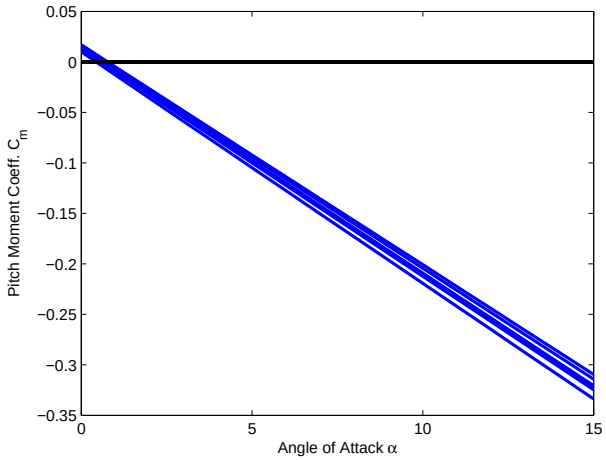

Figure 4: Pitching moment coefficientC_M versus angle of attack α. Center of gravity varying with flight scenarios.

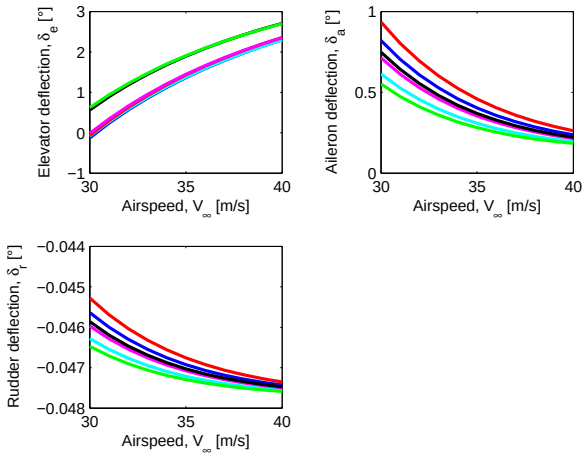

Figure 5: Control surface deflection variation with airspeed.
Blue = Scen. 1, Cyan = Scen. 2, Red = Scen. 3, Magenta = Scen. 4, Black = Scen. 5, Green = Scen. 6.

5 Conclusion

From the comparison of the matrices and the eigenvalues it can be concluded that the accuracy of the longitudinal system matrix is fairly high while the accuracy of the lateral system matrix is very high. Both system matrices generated from the FDM are thus proven to give sufficiently good results indicating that the modelling of the UAV performs well to its purpose. The two different verification methods stated above give promising indication of accuracy of the coded flight dynamics model.

Analyzing the original design we can see that the UAV is not stable in longitudinal motion due to negative damping of the Phugoid mode. Further analysis shows that the design changes suggested above increase the stability of the UAV and it can be determined that with the design changes the UAV meets the requirements form EASA and FAA as well as MIL-F-8785C. It could therefore be concluded that by adding an ballast weight to the fuselage the stability of the Phugoid is increased. It can also be concluded that more forward positioned center of gravity (large static margin) increases the short period natural frequency while more aft positioned center of gravity (small static margin) reduces the short period frequency. This can be explained as decreasing or increasing the pitch moment of inertia I_y, making the movement slow or rapid. Further analysis in improvements of the dynamic stability can be made since a increase in weight is not a completely satisfying improvement. Suggestion of improvements that could be investigated, is to add balance weights in the tail booms of the UAV.

By looking at C_M variation with α we notice the negative slope of the graph and can therefore conclude that the Black Kite is statically stable in pitch. As explained in the above Section.

Lastly when examining the controllability of the UAV we can see that to improve manoeuvrability the area of the elevators could be decreased. By doing this the deflection angle of the surface will operate within a wider range making the plane easier to control. This is because a smaller area will make the airplane less sensitive to disturbances in the angle of deflection. As stated earlier the horizontal stabilizer is mounted with a 3° negative inclination angle. To reduce trim drag the inclination angle could be decreased. This will make the elevators operate around 0° deflection angle. As a final conclusion; trim tabs could be mounted at the rudders to trim the UAV. By doing this the rudders would not be used to trim the UAV since they operate with a very trim limited interval.

6 Future Work

In order to improve the accuracy of the analysis a more detailed mass distribution estimation can be made. This will also give trim flight conditions with a closer match to the actual UAV.

The aerodynamic design changes; decreased area in control surfaces and the use of trim tabs for the rudders, must be further analyzed. This can be done by either a new aerodynamic analysis or wind tunnel testing with a modified model. New aerodynamic coefficients will be derived to verify the improvement of the design of the UAV. The analysis will also determine how much the area of the control surfaces have to be decreased.

As an alternative to the added balance weigh in the aft the effect of balance weights in the tail booms of the UAV can be investigated. This can reduce the amount of added weight.